The photoionization of ammonia revisited.

The vibrational autoionization of NH_3 and its three isotopomers in the 10-12 eV photon energy range

R. Locht, B. Leyh

Département de Chimie Générale et de Chimie Physique, Institut de Chimie, Bât. B6, Université de Liège, Sart-Tilman par B-4000 Liège 1, Belgium

W. Denzer, G. Hagenow and H. Baumgärtel

Institut für Physikalische und Theoretische Chemie, Freie Universität Berlin, Takustrasse 3, W-1000 Berlin 33,

Germany

Abstract

The photoionization efficiency curves of NH_3 and its three isotopomers have been investigated in the photon energy range of the first ionized state. From the analysis of the corresponding vibrational structure, wavenumbers (ω_e) and anharmonicity constants ($\omega_e x_e$) are deduced. The detailed investigation of the abundant autoionization structure tends to show the adiabatic ionization energy to be 10.072 ± 0.010 eV for NH_3, NH_2D and NHD_2 and 10.083 ± 0.010 eV for ND_3. All autoionization features were classified in vibrational progressions (v_2 bending mode) belonging to $n$sa$_1$ (or nd) and $n$pe (n=5, 6, 7) Rydberg series. Vibrational autoionization occurs through Δv transitions up to -9. A qualitative analysis of the intensity distribution of these series strongly supports that transitions involving odd Δv values are favoured. This observation can be understood by applying group theoretical considerations to the theory of vibrational autoionization.

1. Introduction

Below the first ionization limit the vibronic spectrum of NH_3 has been abundantly investigated by numerous workers using various techniques [1-8]. It is generally well established that all the ammonia electronic excited states are of Rydberg character arising from the excitation of one of the nitrogen non-bonding lone pair electrons. The dominant features in these spectra are long vibrational progressions in the v_2 inversion mode arising because the excited states are planar whereas the ground state is pyramidal.

Few investigations of these spectra were extended above the first ionization limit [3,4,7,8]. The most salient feature is the extension of more or less well resolved vibrational progressions up to about 10.8 eV (115 nm) vanishing in a continuum.

Photodissociation of NH_3 in the vacuum UV region into neutral species, e.g. NH_2 and NH, has also been investigated both experimentally and theoretically [9-11]. Emission thresholds for photodissociation were measured.

In the framework of our dissociative ionization study of NH_3 by electron impact [12] and photoionization [13], the contribution of autoionization was shown to play a role. However autoionization in this molecule has scarcely been investigated [14].

The aim of this paper is to report about the autoionization of NH_3 investigated first in the 10-12 eV photon energy range. The present study has been extended to the examination of this phenomenon in the three isotopomers NH_2D, NHD_2 and ND_3. The abovementioned energy range lying below the lowest appearance energy for dissociative photoionization of NH_3 into the NH_2^+ +H channel, the photoionization mass spectrometric technique has been used.

2. Experimental

The experimental setup used in the present experiment is described in detail in a previous paper [15]. Synchrotron radiation provided by the electron storage ring BESSY (Berlin) was used as a light source. It was

dispersed by a 1 meter NIM-monochromator (McPherson 225) equipped with a 1200 ℓ/mm grating. The entrance and exit slits were set to give a resolution of about 0.2 nm. The absolute calibration of the wavelength was better than ±0.2 nm.

The dispersed photon flux passed through an ion chamber and has been measured by a sodium salicylate sensitized photomultiplier. The produced photoions are mass analyzed in a quadrupole mass filter and detected by a channeltron multiplier. The pho-toion yield is continuously normalized to the photon flux.

The sample pressure of 10^{-5} mbar in the ionization region is maintained below 10^{-7} mbar in the monochromator by differential pumping.

The NH_3 sample gas of 99.99% purity was used without further purification. A sample of a mixture ND_3, NH_2D and NHD_2 was obtained from Merck, Sharp and Dohme.

3. Experimental results

Typical photoionization efficiency curves, measured between 9.77-11.80 eV (105-127 nm) photon energy, for the four molecular ions NH_3^+, NH_2D^+, NHD_2^+ and ND_3^+ are displayed in figs. 1 and 2.

An abundant and fairly well resolved autoioniza-tion structure, superposed on a more or less distinguishable "step shaped" ionization continuum, is observed. Very noteworthy is the drastic isotope effect on the shape and intensity of the autoionization structure. Whereas the presence of the underlying step-like continuum is obvious in the deuterated species, it is rather difficult to observe in NH_3. Furthermore, in the low energy range of 9.9-10.0 eV. (123.98-125.2 nm) very weak features are detected in ND_3^+. These are even weaker in NHD_2^+ and are almost not detectable in NH_2D^+ and NH_3^+.

To determine the shape and the structure of the underlying ionization continuum, the photoion yield curves were apodized and filtered by fast Fourier transform to quench the autoionization structure. The yield curves handled in this way were numerically differentiated. A simulated photoelectron spectrum is obtained for the four isotopic species. The result is shown in fig. 3.

Fig. 1. *The photoionization efficiency curves of NH_3 and ND_3. Vertical bars indicate the adiabatic ionization energy. The ND_3^+ ion signal is amplified in the threshold region.*
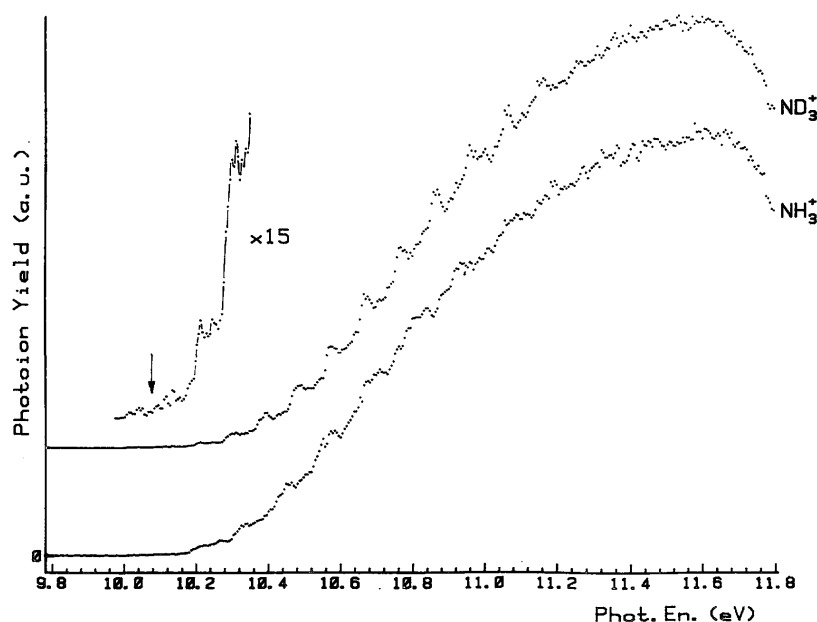
Fig. 2. *The photoionization efficiency curves of NH₂D and NHD₂. Vertical bars indicate the adiabatic ionization energy. The NHD₂⁺ ion signal is amplified in the threshold region.*
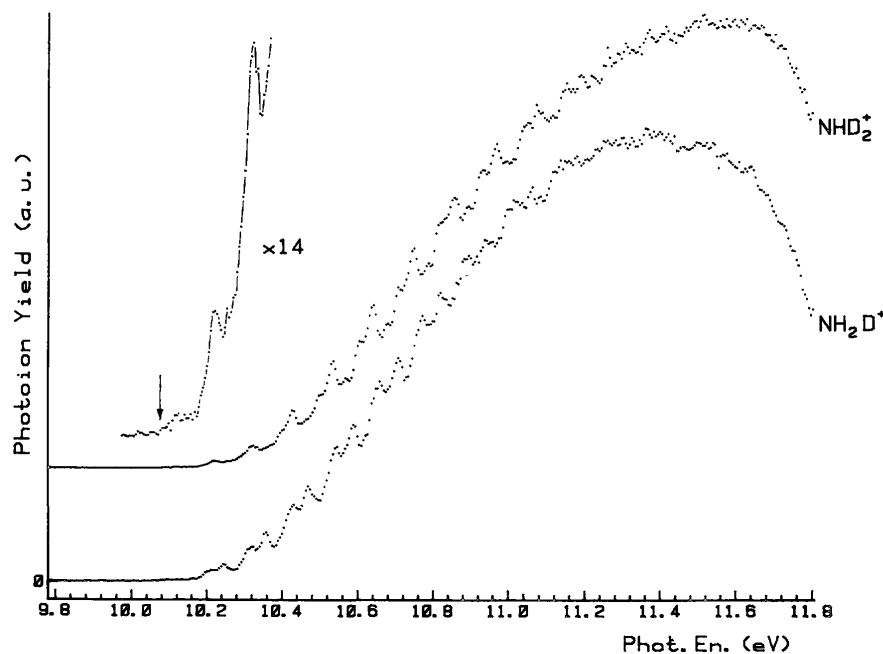
The well known vibrational structure of the ground electronic state of ionized ammonia is observed. The ionization energies deduced from the present work are compared to photoelectron spectroscopic results [16,17] in table 1 in the case of NH_3^+ and ND_3^+. The same data obtained for NH_2D^+ and NHD_2^+ are gathered in table 2.

To enhance the autoionization structure, the filtered ionization efficiency curves are subtracted from the original photoion yield curves. The results obtained for the four isotopomers are shown in figs. 4-7.

The autoionization spectra show remarkable differences for the four isotopic species investigated in this work. For each of these species several vibrational progressions are observed and classified as shown in tables 3-6 and inserted in figs. 4-7. The present results are compared to the most recent electron energy-loss spectroscopic data for NH_3^+ [8].

4. Discussion

4.1. The simulated photoelectron spectra

As shown in table 1 the present photoionization results compare fairly well with the photoelectron spectroscopic data for NH_3^+ [16] and ND_3^+ [17]. However, for ND_3^+ a lower lying level at 10.083 ±0.010 eV has been observed in the present work. This point will be discussed in the next section.

In the four spectra at least thirteen vibronic transitions have been identified and should correspond to the excitation of the same v_2 bending vibrational mode producing the inversion of ammonia [16]. For the four molecular ions a more or less regular increase of the vibrational spacing is observed and has to be related to a negative anharmonicity [16].

The experimental data have been fitted to the following equation [18]

$$E_v = E_0 + (v + 1/2)hc\omega_e - (v+1/2)^2 hc\omega_e x_e, \qquad (1)$$

where x_e/ω_e=constant and where E_v, E_0, v, h, c, ω_e and x_e have the usual meaning. The ratio x_e/ω_e can be assumed to be constant for the four isotopic species. From a first best fit of the experimental data to eq. (1), without any

constraint on E_0, ω_e and $\omega_e x_e$, a ratio

$$-x_e/hc\omega_e = (8.17 \pm 0.58) \times 10^{-2} \ (eV)^{-1}$$

is obtained for NH_2D^+, NHD_2^+ and ND_3^+. For NH_3^+ the value showed a stronger deviation. By inserting this value of x_e/ω_e into eq. (1) a new best fit to the experimental data has been attempted with the constraint that x_e/ω_e remains constant. The results are summarized in table 7.

Fig. 3. *The first derivative of the filtered (see text) ionization efficiency curves of NH₃, NH₂D, NHD₂ and ND₃. Vertical bars locate the adiabatic ionization energy.*
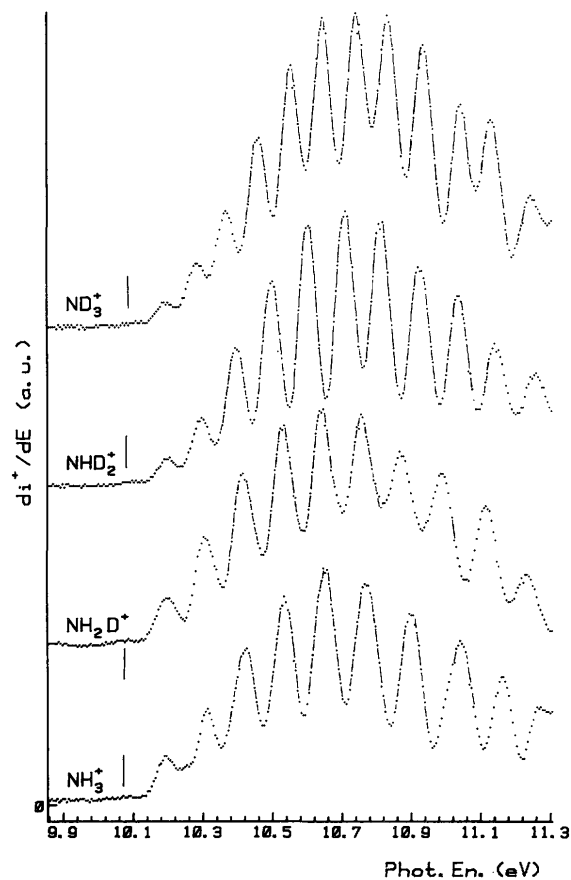
An identical treatment has been applied to the experimental data of Rabalais et al. [16] and Weiss et al. [17]. The results are introduced in table 7. In this table the expected ω_e values are included, as calculated for a valence-force field potential [19] which gives ratios

$$\omega_e(ND_3^+) : \omega_e(NHD_2^+) : \omega_e(NH_2D^+) : \omega_e(NH_3^+)$$

$$= 1 : 1.11 : 1.211 : 1.304 \ .$$

4.2. The adiabatic ionization energy

As shown in figs. 1-3 and in tables 1 and 2, a first ionization energy is measured at 10.072 ±0.010 eV for NH₃, NH₂D, and NHD₂ and at 10.083 ± 0.010 eV for ND₃. For NH₃ the lowest onset measured in this work is in very good agreement with the value published by Rabalais et al. [16], i.e. 10.073 eV. However, these authors mention that "the origin of the band at the lowest energy is uncertain. It may be the 0←0 band or a hot band enhanced by a high Franck-Condon factor". If the peak at 10.073 eV is assumed to correspond to the hot band, the intensity ratio, as measured by the ratio of the peak height between the "hot band" and the next vibrational

level is about 0.2 in the photoelectron spectrum [16].

In the photoionization efficiency curves this ratio can be obtained by measuring the relative height of the "step"-function as far as it can be estimated. In spite of the weakness of the signal in the onset region, a ratio of the first two levels for the four isotopic species investigated in this work, is obtained: $(0.2 \pm 0.05)_{ND_3^+}$; $(0.14 \pm 0.02)_{NHD_2^+}$; $(0.14 \pm 0.02)_{NH_2D^+}$; $(0.15 \pm 0.05)_{NH_3^+}$.

Ågren et al. [20] performed Franck-Condon factor calculations with the data of Rabalais et al. [16]. They ascribed the first band to the adiabatic ionization energy of NH_3. However, Botschwina [21] revised these calculations and concluded that the band at 10.181 eV should correspond to the adiabatic ionization energy.

If the lowest level at about 10.07 eV is assumed to be a hot band, and that at about 10.18 eV is ascribed to the $0 \leftarrow 0$ transition, the intensity ratio is expected to closely reflect the relative population of $v—1$ to $v=0$ levels in the ground electronic state of the molecule. For NH_3 and ND_3 at 300 K the relative population of the $v=1$ bending vibrational level in the molecular ground state would be 1.3×10^{-2} and 3.4×10^{-2} with respect to the ground vibrational level $v=0$, respectively. These ratios do not account for either those measured by photoelectron spectroscopy or by photoionization. There is no argument for a sudden modification of the Franck-Condon factor for the $0 \leftarrow 1$ transition with respect to the $0 \leftarrow 0$ transition. A further argument favouring the present interpretation of the 10.07 eV onset as corresponding to the $0 \leftarrow 0$ transition is found in the photoionization efficiency curves.

Table 1. *Ionization energies (eV) for $\tilde{X}\,^2A_1$, $v \leftarrow \tilde{X}\,^1A_1$, $v=0$ in NH_3 and ND_3 and comparison with photoelectron spectroscopy*

v	NH₃		ND₃	
	this work (± 0.010eV)	ref. [16] (± 0.005 eV)	this work (± 0.010eV)	ref. [17] (± 0.005 eV)
0	10.072	10.073	10.083	-
1	10.191	10.183	10.185	10.180
2	10.309	10.291	10.277	10.290
3	10.422	10.411	10.363	10.380
4	10.530	10.531	10.460	10.473
5	10.643	10.652	10.551	10.581
6	10.767	10.772	10.643	10.664
7	10.896	10.911	10.740	10.762
8	11.036	11.038	10.831	10.842
9	11.160	11.158	10.934	10.942
10	11.289	11.291	11.041	11.039
11	11.434	11.430	11.128	11.141
12	11.564	11.569	11.240	11.246
13	-	11.705	(11.327) [a]	11.331
14	-	11.838	(11.461) [a]	11.443
15	-	11.974	-	-
16	-	12.110	-	-
17	-	12.253	-	-

[a] In parentheses: less accurate values.

Anticipating the discussion of the autoionization spectra (see next section), the detection of very weak structures in ND_3^+ and NHD_2^+ below the assumed lowest ionization energy has to be mentioned. The intensity of these features falls in the background signal for NH_2D^+ and NH_3^+. As shown in tables 3-6 these structures fit fairly well into Rydberg series and will be ascribed to autoionization processes to the $0 \leftarrow 1$ transition. The intensity decrease of the autoionization features with isotopic substitution is qualitatively accounted for by the relative population of the $v=1$ level of the v_2 bending mode in the different isotopomers.

With the hypothesis assuming the adiabatic ionization energy at 10.072 eV (or 10.083 eV) in NH_3 (or ND_3) to be the $0 \leftarrow 1$ hot band, the present features would have to be assigned to autoionization processes to the $0 \leftarrow 2$ transition. The relative population of NH_3 *(v=2)* and ND_3 *(v=2)* are 1.85×10^{-4} and 1.18×10^{-3}. The intensity ratio of the most prominent autoionization features in ND_3^+ below and above 10.083 eV is about 0.2

which is far too large with respect to the expected value.

Table 2. *Ionization energies (eV) for* $\widetilde{X}\,^2A_1$, $v \leftarrow \widetilde{X}\,^1A_1$, $v=0$ in NH_2D and NHD_2

v	NH₂D (± 0.010 eV)	NHD₂ (± 0.010 eV)
0	10.072	10.072
1	10.191	10.191
2	10.298	10.293
3	10.406	10.390
4	10.524	10.497
5	10.637	10.600
6	10.751	10.708
7	10.864	10.810
8	10.988	10.918
9	11.111	11.036
10	11.230	11.138
11	(11.348) [a]	11.257
12	(11.488) [a]	(11.348) [a]
13	-	(11.472) [a]

[a] In parentheses: less accurate values.

Fig. 4. *The autoionization spectrum of NH₃. The vibrational progressions belonging to the four Rydberg transitions are indicated by vertical bars.*
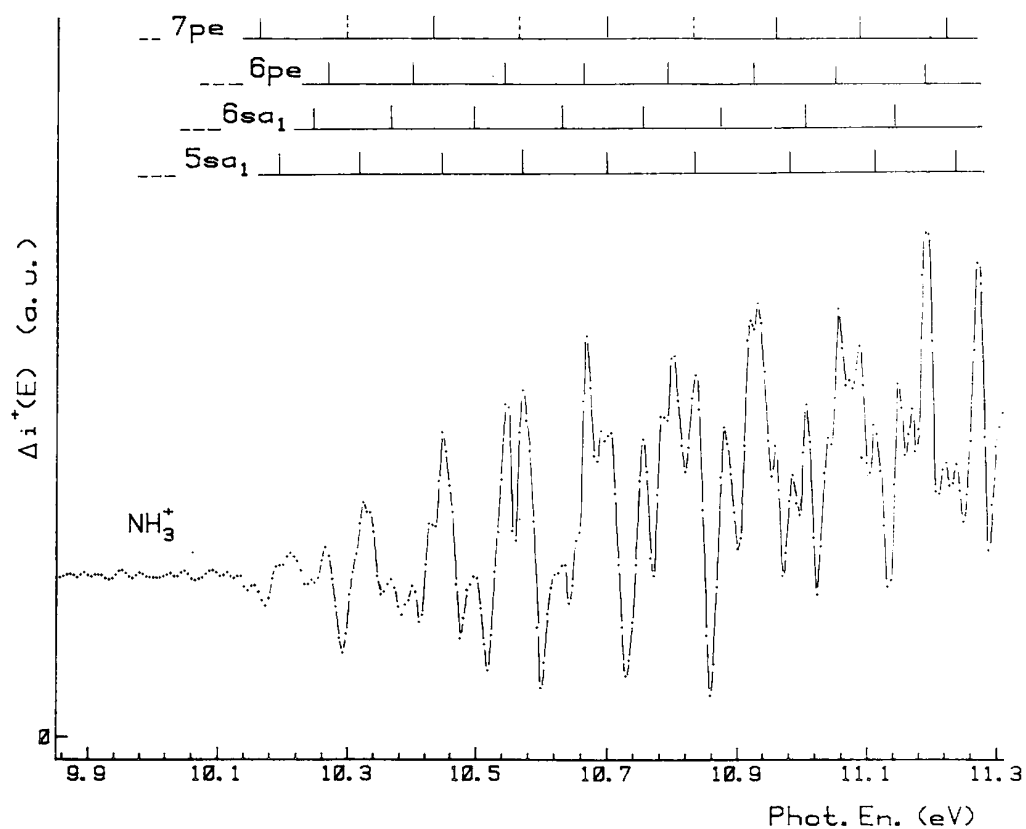
Fig. 5. *The autoionization spectrum of NH$_2$D. The vibrational progressions belonging to the observed Rydberg transitions are indicated by vertical bars.*
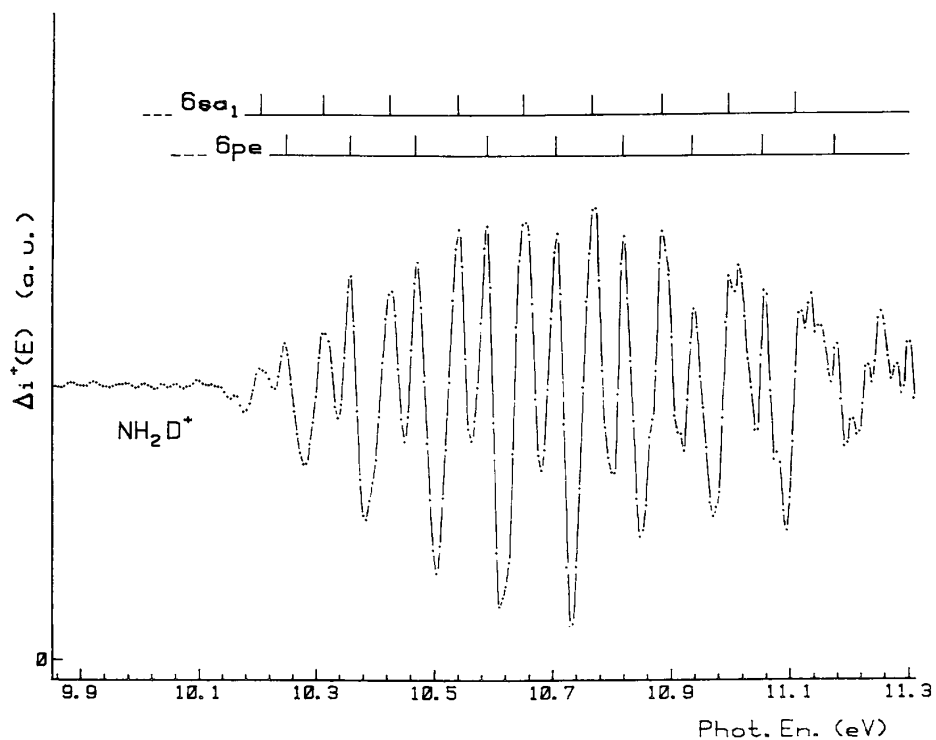
Fig. 6. *The autoionization spectrum of NHD$_2$. The vibrational progressions belonging to the observed Rydberg transitions are indicated by vertical bars.*
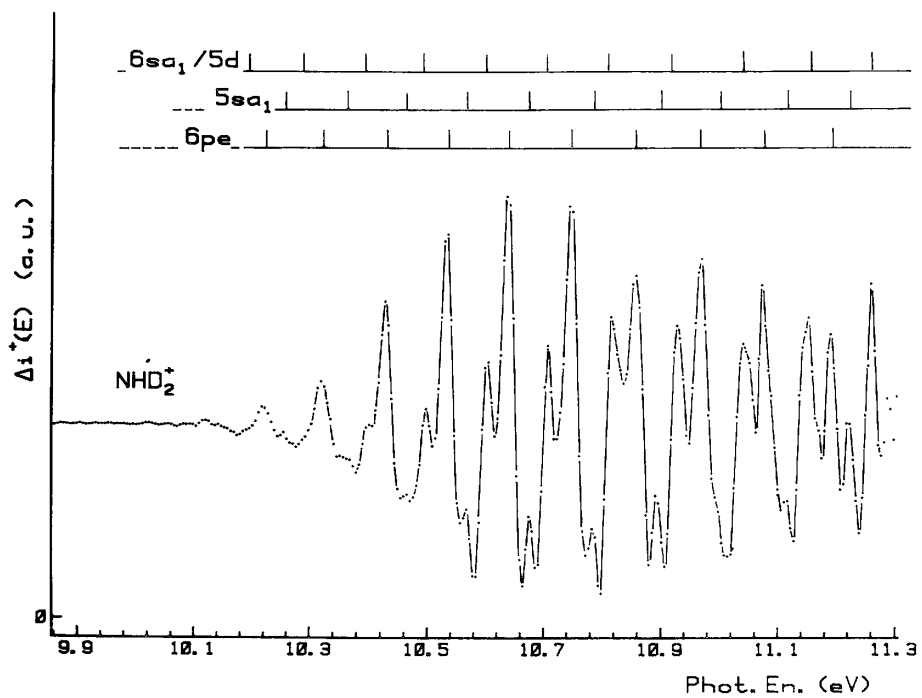
Fig. 7. *The autoionization spectrum of ND$_3$. The vibrational progressions belonging to the observed Rydberg transitions are indicated by vertical bars.*
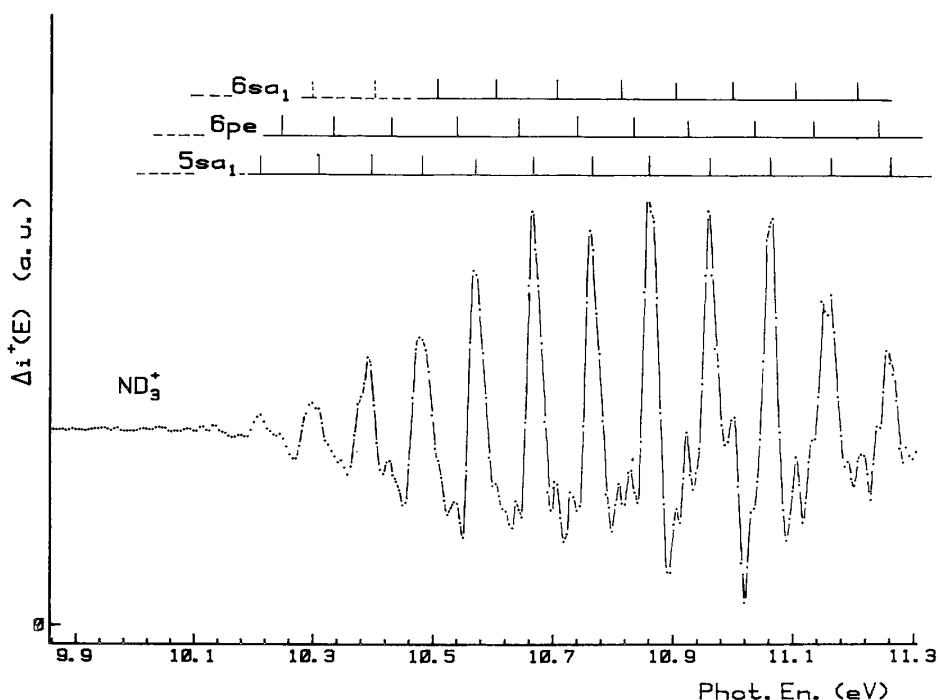

4.3. The autoionization spectra

The electronic configuration of the ground state of ammonia in the C_{3v} symmetry is $(1a_1)^2(2a_1)^2(1e)^4(3a_1)^2\ \tilde{X}\ {}^1A_1$ [22]. The vibronic spectrum is almost only generated by promoting the $3a_1$ electron to ($n$sa$_1$), ($n$pa$_1$), ($n$pe) or nd orbitals. The depletion of the 3a, orbital leads to excited states where the molecule has a planar geometry [20]. Photoabsorption [1-6] and electron energy-loss spectra [7,8] show a series of excited electronic states, each being characterized by only one vibrational progression and assigned to the v_2 inversion bending mode [1-8]. All these states, of Rydberg character (noted in the literature by $\tilde{A}$ to $\tilde{H}$), have been assigned [1-8]. A number of these states were analyzed above the ionization limit of 10.072 eV, e.g. the states designated by $\tilde{D}$, $\tilde{E}$, $\tilde{F}$, $\tilde{G}$) and $\tilde{H}$ states [3,4,7,8].

To analyze the present results the Rydberg formula has been used

$$E_v^{\text{Rydb}} = IE_v - R/(n-\delta)^2 \ ,$$

where E_v^{Rydb} is the energy of the Rydberg vibronic level, IE_V is the energy of the vibrational level v of the molecular ion, R is the Rydberg constant, n is the principal quantum number and δ is the quantum defect. The magnitude of this parameter is strongly bound to the nature of the Rydberg orbital. From previous analyses of the electronic spectra in NH$_3$ the following values of J have been proposed [3,4,23]:

$$\delta(3\text{sa}_1) = 1.25; \ \delta(n\text{sa}_1) = 1.02 \ (n>3);$$

$$\delta(n\text{pe}) = 0.8; \ \delta = (n\text{pa}_1) = 0.54; \ \delta(n\text{d}) \simeq 0.$$

For clarity, in the following discussion the autoionization spectra of the four isotopomers will be discussed separately.

Table 3. *Autoionization spectrum of NH_3: energy (eV), quantum defect (δ), principal quantum number (n), term value (T) (eV) and calculated convergence limit (eV). Comparison with electron energy-loss spectroscopy (EELS) [8] and photoelectron spectroscopy [16]. The estimated error on the present data is $\pm$ 0.010 eV and on EELS data $\pm$ 0.005 eV [8]*

v		NH_3		NH_3^+		Assignt.
		P.I.	EELS [8]	Calc.	Obs. [16]	
A	$(7)^{a)}$	$(10.045)^{a)}$	10.055	(10.904)	10.911	δ =1.02
	8	10.191	10.186	11.050	11.038	$n = 5$
	9	10.320	10.320	11.179	11.158	T=0.859
	10	10.444	10.450	11.303	11.291	$5sa_1$
	11	10.569	10.581	11.428	11.430	
	12	10.701	10.714	11.560	11.569	
	13	10.832	10.845	11.691	11.705	
	14	10.982	10.974	11.841	11.838	
	15	11.106	-	11.965	11.974	
	16	11.236	-	12.095	12.110	
B	5	10.110	10.117	10.658	10.652	δ =1.02
	6	10.239	10.243	10.787	10.772	$n = 5$
	7	10.363	10.374	10.911	10.911	$T = 0.548$
	8	10.492	10.505	11.040	11.038	$6sa_1$
	9	10.632	10.634	11.180	11.158	
	10	10.751	10.765	11.300	11.291	
	11	10.875	10.914	11.423	11.430	
	12	11.003	-	11.551	11.569	
	13	11.144	-	11.692	11.705	
	14	11.266	-	11.814	11.838	
C	5	10.153	10.150	10.664	10.652	δ =0.84
	6	10.261	10.274	10.772	10.772	$n = 6$
	7	10.395	10.400	10.906	10.911	T=0.511
	8	10.541	10.528	11.052	11.038	6pe
	9	10.664	10.657	11.175	11.158	
	10	10.783	10.786	11.294	11.291	
	11	10.928	-	11.439	11.430	
	12	11.052	-	11.563	11.569	
	13	11.187	-	11.698	11.705	
D	6	10.422	_	10.775	10.772	δ =0.80
	7	-	-	-	10.911	n=7
	8	10.697	-	11.050	11.038	T=0.353
	9	-	-	-	11.158	7pe
	10	10.956	-	11.310	11.291	
	11	11.084	-	11.438	11.430	
	12	11.219	-	11.573	11.569	

a) In parentheses: less accurate values.

4.3.1. Ammonia-h_3

For NH_3 two Rydberg series have been identified, i.e. $nsa_1\leftarrow 3a_1$ ($n = 5,\ 6$) and $npe\leftarrow 3a_1$ ($n = 6,\ 7$), as shown in table 3. Except the 7pe state, all other states have been observed previously, i.e. the $5sa_1$, the $6sa_1$, and the 6pe noted in the literature by $\widetilde{E}$, $\widetilde{H}$ and ($\widetilde{F}$,$\widetilde{G}$), respectively. However, for these vibrational progressions a few more levels could be identified. The very weak feature at 10.045 eV could be the most intense member of a residue of a hot band transition $5sa_1$ $(v=7)\leftarrow v=1$. It has to be noted that the accuracy of the present data is obviously not sufficient to distinguish s- and d-type orbitals for higher n values. Furthermore, it has to be

expected that in the energy range covered in this work s- and d-type Rydberg states will probably strongly mix.

Table 4. *Autoionization spectrum of NH$_2$D: energy (eV), quantum defect (δ), principal quantum number (n), term value (T) (eV). Calculated and observed convergence limit (eV). The estimated error on the present data is ±0.010 eV*

	v	NH$_2$D	NH$_2$D$^+$		Assignt.
			Calc.	**Obs.**	
A	5	10.088	10.636	10.637	$\delta = 1.02$
	6	10.196	10.744	10.751	$n = 6$
	7	10.306	10.854	10.864	$T = 0.548$
	8	10.419	10.967	1.0988	6sa$_1$
	9	10.535	11.083	11.111	
	10	10.646	11.194	11.230	
	11	10.764	11.312	(11.348) [a]	
	12	10.880	11.428	(11.488) [a]	
	13	10.993	11.541	-	
	14	11.111	11.659	-	
B	5	10.131	10.650	10.637	$\delta = 0.88$
	6	10.239	10.758	10.751	$n = 6$
	7	10.352	10.871	10.864	$T = 0.519$
	8	10.465	10.984	10.988	6pe
	9	10.584	11.103	11.111	
	10	10.702	11.221	11.230	
	11	10.815	11.334	(11.348) [a]	
	12	10.934	11.453	(11.488) [a]	
	13	11.052	11.571	-	

[a] In parentheses: less accurate values.

For each of these series a long vibrational progression has been observed fitting, in most cases, in series already observed previously. For the 7pe series only the higher part of the progression is observed, the lower members being probably buried under the more intense members of lower energetic states. Table 3 shows good agreement between the present pho-toionization work and electron energy-loss spectroscopy [8]. Furthermore, the calculated convergence limit for each vibrational progression is in good agreement with the photoelectron spectroscopic data of Rabalais et al. [16].

In the four vibrational progressions observed in this work no significant tendency is observed to increase or decrease of the spacing between adjacent levels. An average vibrational wavenumber $\overline{\omega}_e$ can be determined for 5sa$_1$ (1056 ± 60 cm^{-1}), 6pe (1064 ± 80 cm^{-1}), 6sa, (1032 ± 60 cm^{-1}) and 7pe (1080 ± 40 cm^{-1}) for vibrational quanta 5<v<16. Considering v>5, by photoabsorption [3,4] and electron impact [8], no noticeable difference is observed between the four Rydberg states and the ω_e value varies from 1030-1070 cm^{-1}.

In table 3 a vibrational quantum number has been assigned to each member of the four progressions. This assignment takes into account the convergence limit of the two Rydberg series to the ground electronic state of the ion for which the adiabatic ionization energy is determined in this work to be 10.072 ±0.010 eV. Consequently, this has the result of a shift of $\Delta v = +1$ with respect to previous works [3,4,8].

Notwithstanding the crowding of the spectrum displayed in fig. 4 a periodicity of the autoionization features strongly suggests vibrational autoionization. In the frame of this picture the 5 sa$_1$ (v) state autoionizes with $\Delta v = -7$ transitions, the 6sa$_1$ (v) and 6pe(v) autoionize with $\Delta v = -5$ and the 7pe(v) state involves $\Delta v = -3$ transitions. These values are the most probable and in the following we only consider these values.

This phenomenon has been investigated in NO [24] and C$_2$H$_2$ [25]. In these systems the Rydberg states involved are characterized by short vibrational progressions and low vibrational quantum numbers. A propensity rule of $\Delta v = -1$ has been proposed for the vibronic transition from the superexcited state to the adjacent ionization continuum. This selection rule would probably hold for the harmonic approximation

Table 5. *Autoionization spectrum of NHD$_2$: energy (eV), quantum defect (δ), principal quantum number (n), term value (T) (eV). Calculated and observed convergence limit (eV). The estimated error on the present data is ±0.010 eV*

	v	NHD$_2$	NHD$_2^+$		Assignt.
			Calc.	Obs.	
A	8	10.077	10.936	10.918	δ=1.02
	9	10.191	11.050	11.036	*n=5*
	10	10.288	11.147	11.138	*T* =0.859
	11	10.396	11.255	11.257	5sa$_1$
	12	10.492	11.351	(11.348) [a]	
	13	10.600	11.459	(11.472) [a]	
	14	10.702	11.561	-	
	15	10.810	11.669	-	
	16	10.923	11.782	-	
	17	11.036	11.859	-	
	18	11.149	12.008	-	
	19	11.256	12.115	-	
B	4	10.018	10.521	10.497	δ=0.80
	5	10.114	10.617	10.600	*n* = 6
	6	10.218	10.721	10.708	*T* = 0.503
	7	10.315	10.818	10.810	6pe
	8	10.422	10.925	10.918	
	9	10.530	11.033	11.036	
	10	10.632	11.135	11.138	
	11	10.740	11.243	11.257	
	12	10.853	11.356	(11.348) [a]	
	13	10.966	11.469	(11.472) [a]	
	14	11.068	11.571	-	
	15	11.187	11.690	-	
	16	11.284	11.787	-	
C	5	10.050	10.626	10.600	δ=0.14
	6	10.137	10.712	10.708	*n* = 5
	7	10.250	10.826	10.810	*T* = 0.576
	8	10.352	10.928	10.918	5d
	9	10.460	11.036	11.036	
	10	10.562	11.138	11.138	
	11	10.670	11.246	11.257	
	12	10.778	11.354	(11.348) [a]	
	13	10.885	11.461	(11.472) [a]	
	14	-	-	-	
	15	11.106	11.682	-	
	16	11.214	11.790	-	

[a] In parentheses: less accurate values.

However, when long vibrational progressions of high vibrational quanta are involved the breakdown of this propensity rule has been demonstrated. In the diatomic case of H$_2$, near threshold, Chupka and Berkowitz [26] showed the occurrence of vibrational autoionization with Δv= - 6 and Δv= - 4 for D-X(6,0) and B"-X(4,0) transitions, respectively.

More relevant to the present work, Berkowitz and Greene [27] measured the photoion yield curve of PF$_3^+$. Their analysis led to the conclusion that vibrational autoionization occurs with Δv< -13, in sharp contrast to the abovementioned theory of vibrational autoionization.

Table 6. *Autoionization spectrum of ND_3: energy (eV), quantum defect (δ), principal quantum number (n), term value (T) (eV) and calculated convergence limit (eV). Comparison with photoelectron spectroscopic data [17]. The estimated error on the present data is ±0.010 eV*

	v	ND_3	ND_3^+		Assignt.
			Calc.	Obs.	
A	8	10.002	10.861	10.842	δ=1.02
	9	10.093	10.952	10.942	n = 5
	10	10.207	11.066	11.039	T=0.859
	11	10.293	11.152	11.141	$5sa_1$
	12	10.385	11.244	11.246	
	13	10.471	11.330	11.331	
	14	10.562	11.421	11.443	
	15	10.659	11.518	-	
	16	10.756	11.615	-	
	17	10.853	11.712	-	
	18	10.956	11.815	-	
	19	11.058	11.917	-	
	20	11.149	12.008	-	
	21	11.252	12.111	-	
B	5	10.039	10.551	10.581	δ=0.84
	6	10.131	10.643	10.664	n = 6
	7	10.239	10.750	10.762	T =O.511
	8	10.325	10.837	10.842	6pe
	9	10.417	10.928	10.942	
	10	10.530	11.042	11.039	
	11	10.632	11.144	11.141	
	12	10.724	11.235	11.246	
	13	10.826	11.337	11.331	
	14	10.918	11.429	11.443	
	15	11.025	11.536	-	
	16	11.128	11.639	-	
	17	11.209	11.720	-	
C	5	10.050	10.598	10.581	δ=1.02
	6	10.115	10.664	10.664	n = 6
	7	-	-	10.762	T= 0.548
	8	-	-	10.842	$6sa_1$
	9	-	-	10.942	
	10	-	-	11.039	
	11	10.600	11.148	11.141	
	12	10.697	11.245	11.246	
	13	10.804	11.352	11.331	
	14	10.902	11.450	11.443	
	15	10.993	11.541	-	
	16	11.100	11.648	-	
	17	11.187	11.735	-	

.

4.3.2. Ammonia-d_3

The autoionization spectrum of ND_3 is displayed in fig. 7 and the autoionization levels are listed in table 6. Two Rydberg series are identified in this spectrum, i.e. $(nsa_1)\leftarrow 3a_1$ ($n = 5, 6$) and $6pe\leftarrow 3a_1$.

Walsh and Warsop [4] and Glownia et al. [5] investigated ND_3 by photoabsorption spectroscopy.

However, their spectral analysis is confined below the ionization limit. In spite of this limitation, the $0\leftarrow0$ transition of the $5sa_1$ band can be estimated and should be observed at 9.224 eV (74398 cm^{-1}) whereas the $1\leftarrow0$ transition would be at 9.336 eV (75301 cm^{-1}). Glownia et al. [5] mention the origin of an $\tilde{E}$ state at 9.335 eV (75458 cm^{-1}). They assigned this state to the 4d orbital ($\delta=0$) instead of the 5s orbital ($\delta=1.02$) [4]. The 5s and 4d being nearly degenerate, these authors argue that transitions to a 4d orbital should be more intense than a transition to a 5s orbital owing to the n^{-3} intensity relationship [14] and the $\Delta l=+1$ propensity rule determined in atomic spectroscopy [28].

Table 7. Molecular constants ω_e and $\omega_e x_e$ determined for NH_3^+, NH_2D^+, NHD_2^+ and ND_3^+

		ω_e (cm^{-1})	$\omega_e x_e$ (cm^{-1})
NH_3^+	this work	890	-8.0
	ref. [16]	904	-8.0
	ref. [17]	926	-6.6
	calc.	914	
NH_2D^+	this work	848	-7.3
	calc.	849	
NHD_2^+	this work	780	-6.2
	calc.	779	
ND_3^+	this work	701	-5.0
	ref. [17]	713	-3.9
	calc.	701 [a]	

[a] Used as reference (see text).

In opposition to the autoionization spectrum of NH_3, the present spectrum is noticeably simpler. It is dominated by one long vibrational progression of the $5sa_1$/4d state which shows a maximum intensity at about $v=16$. The vibrational progression associated with the transition to $6sa_1$ and 6pe orbitals have an intensity of about 15% of that of the $5sa_1$ transition. The vibrational wavenumber of the $5sa_1$/4d state shows a negative anharmonicity: for $8<v<16$ $\omega_c=750\pm50$cm^{-1} and for $v>16$ $\omega_e=822\pm10$cm^{-1}. The vibrational progressions of $6sa_1$ and 6pe would be characterized by an average $\overline{\omega}_e=787\pm70$ cm^{-1} and 789 ± 64 cm^{-1}, respectively. Characterizing the observed Rydberg series of ND_3 by an $\omega_e=790\pm40$ cm^{-1} and taking for NH_3 an $\omega_e=1060\pm30$ cm^{-1}, a ratio $\omega_{ND3}/\omega_{NH3}=0.75\pm0.06$ is obtained whereas the valence-force field potential predicts a value of 0.767.

Noteworthy is that for the most intense $5sa_1$/4d state the autoionizing transition occurs with an odd $\Delta v=-5$ whereas the other two superexcited 6pe and $6sa_1$ states decay with an even $\Delta v=-6$. On the other hand the observed intensity differences are not accounted for by the ratios given by the n^{-3} rule.

The convergence limit of the Rydberg series is a further argument for the assignments presented in table 6. A satisfactory agreement is found between the vibrational energy of the ion by the Rydberg formula and the experimental data of Weiss et al. [17] obtained by photoelectron spectroscopy.

It has finally to be mentioned that for the three Rydberg states weak structures, ascribed to hot band autoionization, are observed. The features at about 10.002 eV, 10.039 eV and 10.055 eV, lying below the adiabatic ionization energy of 10.083 eV, could be assigned to $5sa_1$ ($v=8$), 6pe ($v=5$) and $6sa_1$ ($v=5$) vibronic states.

4.3.3. Ammonia-d_2

The autoionization spectrum of NHD_2 is shown in fig. 6 and the autoionization levels are listed in table 5. For this isotopomer three Rydberg series are probably observed, i.e. $5sa_1\leftarrow3a_1$, $6pe\leftarrow3a_1$ and $5d\leftarrow3a_1$. For the latter series the experimental results are best fitted by using a quantum defect $\delta=0.14$ though a $\delta(nd)\simeq0$ is expected.

Walsh and Warsop [4] investigated the photoabsorption spectrum of NHD_2 but only below the ionization limit. No energy values are explicitly mentioned.

The autoionization spectrum of NHD_2 is dominated by a vibrational progression ascribed to the $6pe \leftarrow 3a_1$ transition which could be characterized by an average $\overline{\omega}_e = 840 \pm 30$ cm^{-1} and a maximum intensity near $v=10$. This Rydberg state autoionizes with an odd $\Delta v = -5$. The $5d \leftarrow 3a_1$ Rydberg state, with an $\omega_e = 847 \pm 50$ cm^{-1}, is of lower intensity and has to decay with an even $\Delta v = -6$.

In spite of being characterized by the lowest principal quantum number, and therefore expected to be the most intense transition, the weakest series of this autoionization spectrum corresponds to $5sa_1 \leftarrow 3a_1$. Vibrational autoionization occurs with an even $\Delta v = -8$. Below $v=14$ this state shows an average $\omega_e = 850 \pm 60$ cm^{-1} and shows a propensity to increase to 895 ± 20 cm^{-1} for $v > 14$. Taking an average wavenumber $\overline{\omega}_e = 870 \pm 30$ cm^{-1} for the observed Rydberg series and $\omega_{eNH3} = 1060 \pm 30$ cm^{-1} (see section 4.3.1) a ratio $\omega_{NHD2}/\omega_{NH3} = 0.82 \pm 0.04$ is calculated and is comparable with 0.852 obtained by the valence-force field potential (see section 4.1).

The convergence limit for each level has been calculated (see table 5). Satisfactory agreement is found between the vibronic energy levels of the NHD_2^+ molecular ion, as determined by the use of the Rydberg formula and measured in the simulated photoelectron spectrum (see table 2) in this work.

4.3.4. Ammonia-d₁

The autoionization spectrum of NH_2D (see fig. 5) is quite similar to that of NH_3 and is made up of only two Rydberg series, i.e. $6sa_1 \leftarrow 3a_1$ and $6pe \leftarrow 3a_1$ of about equal intensity.

Walsh and Warsop [4] mention the study of this molecule in their photoabsorption work. However, no energy values are listed in the present energy range of interest.

The vibrational progression associated with the $6sa_1$ and the $6pe$ series could be characterized by $\omega_e = 903 \pm 20$ cm^{-1} and 927 ± 30 cm^{-1}, respectively, and the ratio $\omega_{NH2D}/\omega_{NH3} = 0.86 \pm 0.05$ has to be compared with 0.929 obtained by the valence-force field potential.

It has finally to be mentioned that both Rydberg states autoionize to the NH_2D^+ continuum with an odd $\Delta v = -5$.

4.3.5. The intensity distributions

Though it is difficult to discuss quantitatively the intensity distribution in the autoionization spectra of the four isotopomers, as mentioned earlier in this report, they exhibit large differences worthy of comment.

These are not related to the symmetry of the molecular systems: NH_3 and ND_3 exhibit the most dramatic differences. On the contrary, there are more similarities between ND_3 and NHD_2 on one hand and NH_3 and NH_2D on the other hand.

There is no correlation between the intensities and the type of (n,l)-orbital involved in the excitation (n^{-3} and $\Delta l = +1$ rules). When observing the spectra of ND_3 and NHD_2, the strongest autoionization levels are the $5sa_1$ and $6pe$ whereas the weakest are the $6pe$ and $5sa_1$, respectively. These observations are summarized in table 8.

Table 8. *Intensities and autoionizing transitions (Av) characterizing the Rydberg series observed for NH_3 and its three isotopomers*

	5sa₁	5d	6sa₁	6pe	7pe
NH₃	s $\Delta v=-1$	-	w $\Delta v=-5$	s $\Delta v=-5$	w $\Delta v=-3$
NH₂D	-	-	s $\Delta v=-5$	s $\Delta v=-5$	-
NHD₂	vw $\Delta v=-S$	w $\Delta v=-6$		s $\Delta v=-5$	-
ND₃	s $\Delta v=-9$	-	vw $\Delta v=-6$	vw $\Delta v=-6$	-

s=strong, w=weak, vw=very weak.

The first correlation to be pointed out from this table, and stressed along the foregoing discussion, is the

parity of Δv during the autoionizing transition: vibrational autoionization involving odd Δv gives almost rise to the largest intensities.

This experimental observation can be understood in the framework of the theory of vibrational autoionization. This type of autoionization couples a discrete state $|\psi_{nv}\rangle$ and a continuum state $|\psi_{Ev'}\rangle$ having the same core electronic wavefunctions but different vibrational wavefunctions. This interaction results from the fact that the potential energy surfaces of the Rydberg state and of the ionic state are not strictly parallel, owing to the bonding (or anti-bonding) character of the Rydberg electron [29,30]. Therefore, the quantum defect δ used in the Rydberg formula (section 4.3) is no longer a constant but varies slowly with the nuclear coordinate Q. Vibrational autoionization has mostly been studied for diatomic molecules in the framework of the MQDT theory [30,31]. In principle at least, the formalism can be extended to a polyatomic situation.

A Taylor expansion of δ about the ionic equilibrium geometry Q_e^+, truncated to the linear term, is given by

$$\delta(Q) = \delta(Q_e^+) + (Q - Q_e^+)(\mathrm{d}\delta/\mathrm{d}Q)_{Q=Q_e^+}.$$

The coupling matrix element between $|\psi_{nv}\rangle$ and I $\psi_{Ev'} >$ can than be written:

$$\langle \psi_{nv} | H | \psi_{Ev'} \rangle = \left(\frac{2R}{n^{*3}} \frac{\mathrm{d}E}{\mathrm{d}n} \right)^{1/2} (\mathrm{d}\delta/\mathrm{d}Q)_{Q=Q_e^+}$$

$$\times \langle v | Q - Q_e^+ | v' \rangle,$$

where $n^* = n - \delta$.

In the case of $N(H, D)_3$, as both the Rydberg and the ionic states are planar, the D_{3h} point group has to be considered. The Q-coordinate is here the out-of-plane bending vibration belonging to the A_2'' representation. The vibrational states $|v\rangle$ and $|v'\rangle$ describe this motion. If $|v\rangle$ and $|v'\rangle$ have the same parity (Δv is even), their product will belong to the totally symmetric A'_1 representation, the integrand to A_2'' and the integral $\langle v | Q - Q_e^+ | v' \rangle$ will vanish. On the other hand, if Δv is odd, the integrand will belong to A_1' and the integral will be different from zero. From these symmetry considerations it has to be concluded that transitions involving odd Av values should be strongly favoured, in agreement with the experimental observations.

Two remarks are worth a short discussion. First, in the harmonic approximation, Av will be limited to -1, owing to the specific properties of the Hermite polynomials [32]. In the present work Av values up to — 9 are observed. This is most probably due to the strong anharmonicity of the potential energy surface of NH_3^+ ($\tilde{X}\,^2A_1$) (see section 4.1), which will manifest itself especially when high v autoionizing levels (up to $v=21$) are involved (see tables 3-6). Secondly, it can be argued that the abovementioned reasoning is only valid if δ varies linearly with Q. Taking into account the quadratic contribution would allow autoionizing transitions involving even Δv values. The fact that such transitions are weaker in the present case (see table 8), tends to support that the quadratic term is less significant than the linear one. It should also be mentioned that, even in the harmonic approximation, higher-order effects can produce small couplings for any Av value. Although such effects have been observed by Dehmer and Chupka [33], they are generally much weaker than the first-order effects.

The differences in the intensity distribution observed in the autoionization spectrum of the four isotopomers have been discussed and justified only in terms of the Δv-parity: however, the isotope effect has explicitly not been considered. This effect could act through the photodissociation of the superexcited states, and has therefore to be considered.

This phenomenon has been investigated in NH_3 [9,10]. In the range of interest in this work, the main dissociation channel is $NH+H_2$. The fluorescence corresponding to $NH(c^1\Pi, b^1\Sigma^+, a^1\Delta)$ has been observed up to 11.3 eV [10]. The rate constant would be expected to be dependent upon isotopic substitution and photodecomposition could compete with autoionization.

However this isotope effect is difficult to analyze mainly because of the interference of several effects.

The involved Rydberg states differ from one isotopomer to the other. When the same superexcited states are involved, e.g. in NH_3 and ND_3, the Δv propensity rule is operative. Furthermore, no symmetry restriction exists between the initial Rydberg states and final states of the abovementioned dissociation products. More detailed experimental data are needed to investigate these phenomena.

Conclusions

The photoionization efficiency curves of NH_3, NH_2D, NHD_2 and ND_3 have been recorded in the 9.7-11.8 eV photon energy range. The detailed investigation of these curves allowed us to suggest a value of the adiabatic ionization energy of the ground ionic state. The corresponding ω_e and $\omega_e x_e$ values, associated with the long v_2 bending mode vibrational progression observed in the yield curves, are deduced for the four species. Within experimental error, good agreement is found between the present experimental results and predicted values for these molecular constants. For NH_3 and ND_3 the results compare very well with photoelectron spectroscopic data.

An abundant autoionization structure is superposed on the ionization continuum. This structure markedly changes with isotopic substitution. It has been analyzed in terms of Rydberg series converging to the first ionization limit. Each series is characterized by a long vibrational (v_2 bending mode) progression. Only in the case of NH_3 a comparison could be made with previous photoabsorption and electron energy-loss spectroscopic data. Energies and wave-numbers are in satisfactory agreement.

These Rydberg states autoionize vibrationally. A close correlation is observed between the parity of the vibrational transition Av and the intensity of the corresponding autoionization process. To odd Δv's correspond the strongest intensities. These observations can be accounted for by symmetry considerations applied to vibrational autoionization theory.

Though not discussed in detail in this work, an isotope effect on the relative intensities of the Rydberg states through their photodissociation into neutral fragments, e.g. $NH(D)+H_2(HD, D_2)$, has to be expected.

Acknowledgement

References

[1] A.B.F. Duncan, Phys. Rev. 47 (1935) 822; A.B.F. Duncan and A.E. Douglas, Phys. Rev. 49 (1936) 211.

[2] A.E. Douglas and J.M. Hollas, Can. J. Phys. 39 (1961) 479; A.E. Douglas, Discussions Faraday Soc. 35 (1963) 158.

[3] K. Watanabe and S.P. Sood, Sci. Light (Tokyo) 14 (1965)36.

[4] A.D. Walsh and P.A. Warsop, Trans. Faraday Soc. 57 (1961) 345.

[5] J.H. Glownia, S.J. Riley, S.D. Colson and G.C. Nieman, J. Chem. Phys. 73 (1980) 4296.

[6] V. Vaida, W. Hess and J.L. Roebber, J. Phys. Chem. 88 (1984) 3397; V. Vaida, M.I. McCarthy, P.C. Engelking, P. Rosmus, H.W. Werner and P. Botschwina, J. Chem. Phys. 86 (1987) 6669.

[7] W.R. Harschbarger, J. Chem. Phys. 54 (1971) 2504.

[8] M. Furlan, M.J. Hubin-Franskin, J. Delwiche, D. Roy and J.E. Collin, J. Chem. Phys. 82 (1985) 1797.

[9] H. Okabe, Photochemistry of Small Molecules (Wiley, New York, 1978).

[10] M. Suto and L.C. Lee, J. Chem. Phys. 78 (1983) 4515.

[11] M.I. McCarthy, P. Rosmus, H.J. Werner, P. Botschwina and V. Vaida, J. Chem. Phys. 86 (1987) 6693.

[12] R. Locht, Ch. Servais, M. Ligot, M. Davister and J. Momigny, Chem. Phys. 125 (1988) 425; R. Locht, Ch. Servais, M. Ligot, F. Derwa and J. Momigny, Chem. Phys. 123 (1988) 443; R. Locht and J. Momigny, Chem. Phys. 127 (1988) 425.

[13] R. Locht, W. Denzer, G. Hagenow and H. Baumgärtel, to be published.

[14] J. Berkowitz, Photoabsorption, Photoionization and Photoelectron Spectroscopy (Academic Press, New York, 1979).

[15] K. Rademann, H.W. Jochims and H. Baumgärtel, J. Phys. Chem. 89 (1985) 3459.

[16] J. Rabalais, L. Karlsson, L.O. Werme, T. Bergmark and K. Siegbanh, J. Chem. Phys. 58 (1973) 3370.

[17] M.J. Weiss, G.W. Lawrence, J. Chem. Phys. 53 (1970) 214.

[18] G. Herzberg, Molecular Spectra and Molecular Structure. I. Spectra of Diatomic Molecules (Van Nostrand, Princeton, 1967).

[19] G. Herzberg, Molecular Spectra and Molecular Structure. II. Infrared and Raman Spectra (Van Nostrand, Princeton, 1945).

[20] H. Ågren, I. Reineck, H. Veenhuizen, R. Maripuu, R. Arneberg and L. Karlsson, Mol. Phys. 45 (1982) 477.

[21] P. Botschwina, Ion and Cluster Ion Spectroscopy and Structure, ed. J.P. Maier (Elsevier, Amsterdam, 1989) p. 83.

[22] G. Herzberg, Molecular Spectra and Molecular Structure. III. Electronic Spectra and Electronic Structure of Polyatomic Molecules (Van Nostrand, Princeton, 1967).

[23] G.R. Wright and C.E. Brion, J. Electron Spectrosc. & Relat. Phenom.4 (1974) 25.

[24] Y. Ono, S.H. Linn, H.F. Prest, C.Y. Ng and E. Miescher, J. Chem. Phys. 73 (1980) 4855. [25] Y. Ono, E.A. Osuch and C.Y. Ng, J. Chem. Phys. 76 (1982) 3905.

[26] W.A. Chupka and J. Berkowitz, J. Chem. Phys. 51 (1969) 4244.

[27] J. Berkowitz and J.P. Greene, J. Chem. Phys. 81 (1984) 4328.

[28] T.M. Dunn, Studies in Chemical Structure and Reactivity, ed. J.H. Ridd (Methuen, London, 1966).

[29] G. Herzberg and Ch. Jungen, J. Mol. Spectry. 41 (1972) 425.

[30] H. Lefebvre-Brion and R.W. Field, Perturbations in the Spectra of Diatomic Molecules (Academic Press, New York, 1986).

[31] Ch. Jungen and D. Dill, J. Chem. Phys. 73 (1980) 3338.

[32] E.B. Wilson, J.C. Decius and P.C. Cross, Molecular Vibrations (Dover, New York, 1983) Appendix III.

[33] P.M. Dehmer and W.A. Chupka, J. Chem. Phys. 65 (1976) 2243.